Threshold displacement energy in GaN: Ab initio molecular dynamics study

H. Y. Xiao, Fei Gao, X. T. Zu, and W. J. Weber

Threshold displacement energy in GaN: *Ab initio* molecular dynamics study

H. Y. Xiao,[1,a)] Fei Gao,[2,b)] X. T. Zu,[1] and W. J. Weber[2]

[1]*Department of Applied Physics, University of Electronic Science and Technology of China, Chengdu 610054, People's Republic of China*
[2]*Pacific Northwest National Laboratory, P.O. Box 999, Richland, Washington 99352, USA*

Large-scale *ab initio* molecular dynamics method has been used to determine the threshold displacement energies E_d along five specific directions and to determine the defect configurations created during low energy events. The E_d shows a significant dependence on direction. The minimum E_d is determined to be 39 eV along the $\langle \bar{1}010 \rangle$ direction for a gallium atom and 17.0 eV along the $\langle \bar{1}010 \rangle$ direction for a nitrogen atom, which are in reasonable agreement with the experimental measurements. The average E_d values determined are 73.2 and 32.4 eV for gallium and nitrogen atoms, respectively. The N defects created at low energy events along different crystallographic directions have a similar configuration (a N–N dumbbell configuration), but various configurations for Ga defects are formed in GaN. © *2009 American Institute of Physics.*
[DOI: 10.1063/1.3153277]

I. INTRODUCTION

In the last few years, GaN has attracted great interest due to its technologically important applications in the fabrication of a range of electronic and photonic devices.[1] In the fabrication of GaN-based devices, ion implantation was proved to be an important technique to introduce dopants in selective areas and to control the dopant concentration over a well-defined depth distribution; however, the successful application of ion-implantation doping requires a fundamental understanding of the production and annealing of irradiation damage in GaN.[2,3] A key physical parameter, relevant to defect production under irradiation, is the threshold displacement energy E_d, which is commonly defined as the minimum kinetic energy transferred to an atom in the lattice from an impinging particle necessary to permanently displace that atom, or an atom of the same species, from its lattice site, thus forming a stable defect. The threshold displacement energy E_d is useful for estimating damage production rates for electrons, neutrons, and light ions, as well as for scaling fast neutron and ion irradiations.[4] It is also an important quantity for enabling Monte Carlo simulations of displacement cascades or for determining defect profiles from implantation doping.[5]

A large number of experimental investigations have been performed to characterize damage accumulation in GaN under ion bombardment.[2,3,6–21] Although several experimental techniques are available to indirectly measure E_d, the nature of the threshold event, which occurs in less than a picosecond, can only be inferred from the resulting primary damage state.[4] Molecular dynamics (MD) simulations were proved to be a valuable tool for understanding the atomic-level defect production mechanisms on the picosecond time scale.[22–25] MD determinations of threshold displacement energies based

on empirical potentials have been successfully carried out on a number of materials such as SiC,[26–31] diamond,[32] MgO,[33] zircon,[34] TiAl,[35] Ni$_3$Al,[36] and vanadium.[37] However, empirical potentials usually give a poor description of the saddle states that the lattice atom must overcome to reach an interstitial state.[5] For SiC, previous studies have shown that there are significant discrepancies among the simulation results due to variations in the potentials employed.[26–31] In the case of GaN, MD simulations with an analytical bond-order potential have also been carried out by Nord *et al.*[25,38] to determine E_d and study damage accumulation during ion beam irradiation; however, both the minimum and average E_d values calculated for gallium are unexpectedly lower than those for nitrogen in contrast to the experimental measurments.[39] Recently, the values for E_d in SiC (Ref. 5) and Si (Ref. 40) have been investigated by *ab initio* MD methods, which provide important insights into defect creation at low energies. In the present study, large-scale ($>$400 atoms) *ab initio* MD methods have been employed to determine E_d in GaN and obtain the defect configurations created by the low energy recoil events. The results are compared with the previous classical MD simulations and the possible consequences on defect evolution and accumulation in GaN are discussed.

II. COMPUTATIONAL APPROACH

All the calculations were performed using the computer program SIESTA.[41] To simulate threshold displacement events and ion-solid interactions, the SIESTA code has been modified to initiate a primary knock-on atom (PKA) at a given direction and kinetic energy, and a variable time step approach has been adapted, which ranges from 0.001 to 1 fs. The interaction between ions and electrons is described using norm conserving Troullier–Martins[42] pseudopotentials factorized in the Kleinman–Bylander form.[43] The reference electronic configurations for the pseudopotentials are $4s^2 4p^1 4d^0$ for a Ga atom and $2s^2 2p^3$ for a N atom. The

a)Electronic mail: hyxiao@uestc.edu.cn.
b)Electronic mail: fei.gao@pnl.gov.
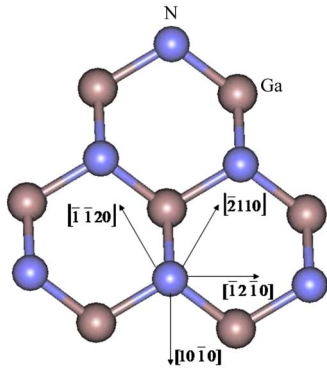
FIG. 1. (Color online) Schematic illustration of the main crystallographic directions in wurtzite GaN. Ga and N atoms are indicated.

pseudopotential core radii for Ga were 2.08, 2.3, and 3.3 bohr for the s, p, and d channels, respectively, and 1.37 bohr for the N s and p channels.[44] The lattice parameters a_0 and c_0 for the wurtzite (hexagonal) GaN were optimized to be 3.24 and 5.255 Å, respectively, which are in excellent agreement with experimental measurements.[45] The localized gradient approximation functional proposed by Perdew and Zunger[46] was used. The valence wave functions were expanded in a basis set of localized atomic orbitals and single-ζ basis sets were used. In this minimal basis set, only one single radial function per angular momentum channel is used. For Ga atoms, the cutoff radii are 5.16 and 6.794 bohr for $4s$ and $4p$ orbitals, respectively, and for N atom the $2s$ and $2p$ cutoff radii are 3.593 and 4.175 bohr, respectively. A cutoff energy of 90 Ry and Γ-point sampling in the Brillouin zone were used in this work. To simulate a recoil event near the threshold energy, the simulation supercell must be large enough to contain the PKA and to prevent interactions between the PKA and the thermostat during the simulation. All the simulations were conducted with a 432 atom cell at constant particle number and volume with periodic boundary conditions imposed along three directions. A variable time step scheme was employed to avoid the instability of the simulations. The crystal was first equilibrated for 1000 time steps ($\sim$1 ps) at 100 K. An atom (Ga or N) was selected as the PKA and it was given a kinetic energy to initiate a recoil event. If no stable Frenkel pair remained at the end of the recoil event, the simulation was restarted at higher recoil energy with an energy increment of 5 eV. Once a stable Frenkel pair was formed, additional five runs were preformed to improve the precision to 1 eV. In wurtzite GaN, the atom arrangements along the $[\bar{1}2\bar{1}0]$, $[\bar{2}110]$, and $[\bar{1}\bar{1}20]$ directions are equivalent to each other. Hence, for each type of atom (Ga and N), only five main crystallographic directions ($[\bar{1}2\bar{1}0]$, $[10\bar{1}0]$, $[\bar{1}010]$, $[0001]$, and $[000\bar{1}]$) were investigated in the present study (as shown in Fig. 1).

III. RESULTS AND DISCUSSION

The threshold displacement energies along the main crystallographic directions and resulting defect configurations for both Ga and N atoms are summarized in Table I. The corresponding defect configurations for N and Ga PKAs are illustrated in Figs. 2 and 3, respectively. As shown in

TABLE I. The calculated threshold displacement energies and the associated created defect configurations. d_{FP}: the Frenkel pair separation; V_{Ga}: a Ga vacancy; V_N: a N vacancy; NN: a nitrogen-nitrogen dumbbell; Ga_O: a Ga octahedral interstitial; Ga_{int}: Ga interstitial.

Direction	E_d (eV)	Defect type	d_{FP} (Å)
N$[\bar{1}2\bar{1}0]$	18.5	V_N+tilted NN$\langle\bar{1}2\bar{1}0\rangle$	3.77
N$[10\bar{1}0]$	41.5	V_N+tilted NN$\langle10\bar{1}0\rangle$	3.54
N$[\bar{1}010]$	17.0	V_N+tilted NN$\langle\bar{1}010\rangle$	3.76
N$[0001]$	78.0	V_N+tilted NN$\langle0001\rangle$	5.29
N$[000\bar{1}]$	77.0	V_N+tilted NN$\langle000\bar{1}\rangle$	7.06
		N sublattice, weighted average: 32.4 eV	
Ga$[\bar{1}2\bar{1}0]$	73.0	V_{Ga}+V_{Ga}+Ga_O+tilted GaGa$\langle\bar{1}2\bar{1}0\rangle$+$V_N$+tilted NN$\langle\bar{1}2\bar{1}0\rangle$	3.67
Ga$[10\bar{1}0]$	87.0	V_{Ga}+Ga_O+V_N+tilted NN$\langle10\bar{1}0\rangle$	1.88
Ga$[\bar{1}010]$	39.0	V_{Ga}+Ga_O	4.62
Ga$[0001]$	85.0	V_{Ga}+V_{Ga}+Ga_O+V_N+V_N+N−Ga−N cluster	3.36
Ga$[000\bar{1}]$	83.0	V_{Ga}+Ga_{int}+V_N+tilted NN$\langle000\bar{1}\rangle$	5.86
		Ga sublattice, weighted average: 73.2 eV	

Table I, the defects created by N PKAs along different crystallographic directions show similar atomic arrangements; however, the recoil events for Ga PKAs result in different defect configurations. In most cases, the minimum E_d leads to the formation of simple Frenkel defects, but some complex defect configurations are observed, particularly for Ga PKAs.

When a kinetic energy below E_d is transferred to a N atom along the $\langle\bar{1}2\bar{1}0\rangle$ direction, the PKA initially moves from its equilibrium location along this direction but then returns to its original position without creating defects. As the kinetic energy is increased to 18.5 eV, the PKA initially moves along the $\langle\bar{1}2\bar{1}0\rangle$ direction to interact with one of its first-neighbor Ga atoms; however, the strong repulsive interaction between the PKA and this Ga atom results in the PKA trajectory shifting toward the nearest tetrahedral site while continuing along the $\langle\bar{1}2\bar{1}0\rangle$ direction. Finally, this N PKA interacts with a third nearest-neighbor N atom to form a tilted NN $\langle\bar{1}2\bar{1}0\rangle$ dumbbell, as shown in Fig. 2(a). Thus, in this case, E_d is 18.5 eV, and the Frenkel pair separation distance d_{FP} is 3.77 Å. Similar threshold event phenomena have been observed for a C recoil along the $\langle100\rangle$ direction in 3C–SiC.[5] For a N PKA along the $\langle10\bar{1}0\rangle$ direction, the mechanism is relatively more complex, and kinetic energies larger than 41.5 eV lead to the N atom overcoming an energy barrier formed by a N and a Ga atom to directly interact with a N atom. This process transfers substantial kinetic energy to the N atom, such that the PKA replaces this N atom, as shown in Fig. 2(b), which continues moving along the same direction and interacts with another N atom to form a tilted NN$\langle10\bar{1}0\rangle$ dumbbell with a separation distance of 3.54 Å from the vacancy formed at the original PKA site. For a N PKA along the $\langle\bar{1}010\rangle$ direction, the E_d determined is 17.0 eV, which is much smaller than that along the $\langle10\bar{1}0\rangle$ direction, but the mechanism is relatively simpler. Along the
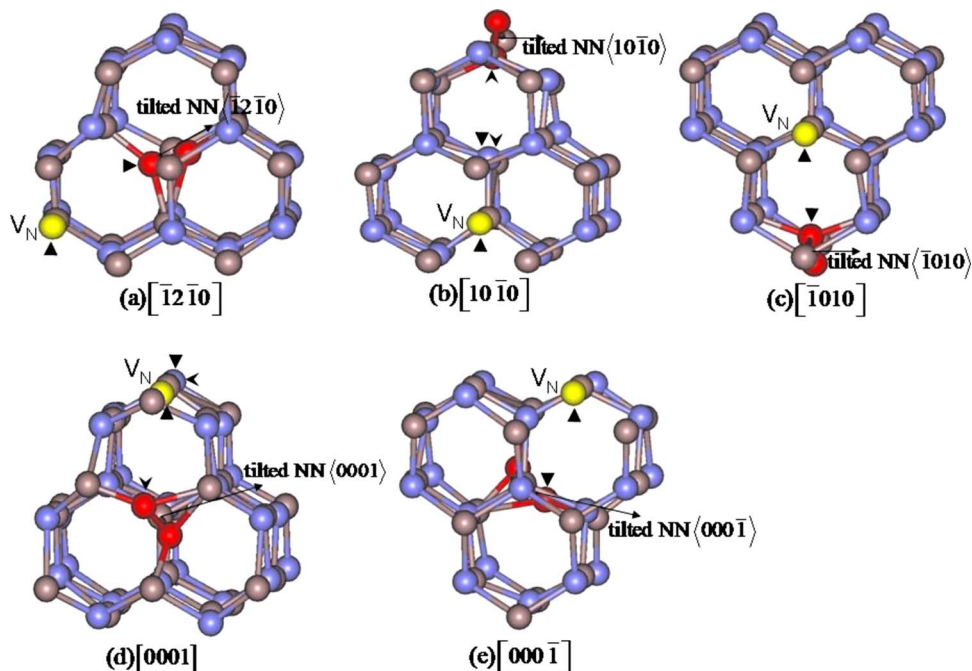
FIG. 2. (Color online) Schematic views of the defect configuration for PKAs on N sublattice in each considered crystallographic direction. The atom types are the same as those in Fig. 1. Black (red) spheres represent N and light gray (yellow) spheres represent N vacancies. The same types of arrows show the position of the corresponding atoms before and after the threshold event.

$\langle \bar{1}010 \rangle$ direction, the N PKA moves at 3.76 Å to directly interact with a N atom to form a tilted NN $\langle \bar{1}010 \rangle$ dumbbell, as shown in Fig. 2(c). In the case of a N PKA along the $\langle 0001 \rangle$ direction, the E_d is determined to be 78.0 eV, which is much higher than along the other three directions considered.

Along this direction, as shown in Fig. 2(d), the N PKA collides with a Ga atom, which receives sufficient energy to move along the same direction and interact with a second N atom. Due to the strong repulsive energy during this process, both the Ga and second N atom reverse direction and move
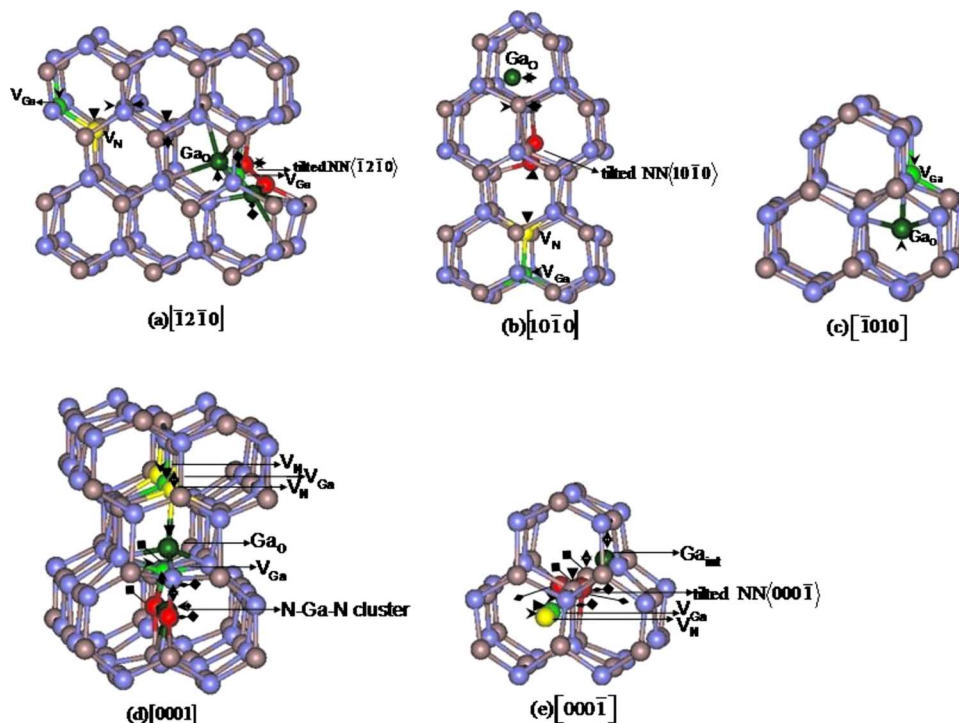
FIG. 3. (Color online) Schematic views of the defect configuration for PKAs on Ga sublattice in each considered crystallographic direction. The atom types are the same as those in Fig. 1. Black and dark gray (red and green) spheres represent N and Ga defects, respectively, and light gray (yellow) and jade-green spheres represent N and Ga vacancies, respectively. The same types of arrows show the position of the corresponding atoms before and after the threshold event.

back along the $\langle 000\bar{1}\rangle$ direction. The Ga atom subsequently returns to its original position without creating defects, and the second N atom overcomes an energy barrier formed by the Ga atom and its nearest-neighbor N atoms and occupies the original position of the N PKA, with a N vacancy now formed in the original site occupied by the second N atom. At the same time, the original interaction between the N PKA and the Ga atom causes the N PKA to move along the $\langle \bar{1}010\rangle$ direction and interact with a third N atom to produce a tilted NN $\langle 0001\rangle$ dumbbell. In the case of a N PKA along the $\langle 000\bar{1}\rangle$ direction, it is interesting to find that the E_d is nearly the same as that of the N PKA along the $\langle 0001\rangle$ direction. When a kinetic energy of 77.0 eV is given to a N atom along the $\langle 000\bar{1}\rangle$ direction, the N PKA collides directly with its nearest-neighbor Ga atom, which moves along the same direction. The strong interaction between these two atoms changes the trajectory of the N PKA, which moves 7.06 Å away from its original position to form a tilted NN$\langle 000\bar{1}\rangle$ dumbbell with a nitrogen atom, as shown in Fig. 2(e). The originally struck Ga atom returns to its original position. It is observed that for all the N PKA recoils along the different directions only nitrogen interstitials and vacancies are created. This is consistent with our previous calculations[47,48] of defect properties in GaN, in which systematic investigations have been performed using different methods and interaction potentials, and the nitrogen defects are shown to be more stable than the Ga defects under nitrogen-rich conditions. It has been shown that the most stable interstitial for nitrogen atoms forms a dumbbell configuration, and all other nitrogen interstitials eventually convert into this configuration at high temperatures.

Similar to the cases of the N recoils, a similar approach has been employed for Ga recoils. For a Ga PKA along the $\langle \bar{1}2\bar{1}0\rangle$ direction, the mechanism is relatively more complicated and the defect configurations are much different as compared to the N$[\bar{1}2\bar{1}0]$ case. In this case, the Ga PKA initially collides with its first-neighbor Ga atom along this direction and occupies its site. The strong repulsive interaction between the replaced Ga atom and its neighboring atoms leads it to move toward its nearest octahedral site, where it forms a stable octahedral interstitial that eventually interacts with another Ga atom to form a tilted GaGa $\langle \bar{1}2\bar{1}0\rangle$ dumbbell, as shown in Fig. 3(a). In addition, the original Ga PKA interacts strongly with a nearest-neighbor N atom, resulting in the N atom moving along the original PKA direction and replacing another N atom. The replaced N atom moves further and interacts with another N atom resulting in the formation of a tilted NN dumbbell, similar to the configuration for the N$[\bar{1}2\bar{1}0]$ case. The corresponding E_d is 73.0 eV. For a E_d of 87 eV along the $\langle 10\bar{1}0\rangle$ direction, the Ga PKA collides directly with its nearest-neighbor N atom and pushes the N atom off its site, leading to a Ga and a N vacancy. The N atom interacts with another nearby N atom, resulting in a defect configuration consisting of a tilted NN $\langle 10\bar{1}0\rangle$ dumbbell. The Ga PKA moves further along the same direction and replaces a Ga atom, which forms a stable gallium inter-

stitial at an octahedral site [see Fig. 3(b)]. For a Ga PKA along the $\langle \bar{1}010\rangle$ direction, the E_d is 39.0 eV. In this case, the Ga PKA moves at 4.62 Å away from its original site along the $\langle \bar{1}010\rangle$ direction and forms a stable gallium interstitial at an octahedral site, as shown in Fig. 3(c). For a Ga PKA along the $\langle 0001\rangle$ direction, complex defect configurations are produced at the threshold displacement event, as shown in Fig. 3(d), where the final defect configuration consists of two Ga vacancies, an octahedral Ga interstitial, two N vacancies, and a N–Ga–N cluster. It is noted that this event produces many displacements on both the Ga and N sublattices at the peak of displacement, much like a local cascade, which may account for the high E_d of 85.0 eV. For a Ga PKA recoil along the $\langle 000\bar{1}\rangle$ direction, the threshold displacement energy of 83.0 eV is very similar to that of the Ga [0001] case. In the Ga $[000\bar{1}]$ case, a displacement sequence along the $\langle 000\bar{1}\rangle$ direction is observed, which results in a defect configuration consisting of one Ga vacancy, one N vacancy, and a Ga interstitial. One N atom is ejected along the $\langle 000\bar{1}\rangle$ direction to form a tilted NN$\langle 000\bar{1}\rangle$ dumbbell [see Fig. 3(e)]. The current simulations have demonstrated that the threshold displacement energies in GaN are anisotropic, which strongly depend on the PKA directions.

Experimentally,[49] gallium nitride light emitting diodes were irradiated at room temperature with electrons in the range between 300 and 1400 keV. While no threshold energy for the nitrogen atom was observed due to the fact that the nitrogen sublattice repairs itself through annealing, a measured value of 19 ± 2 eV for the Ga atom is reported. By analyzing the transport properties of electron-irradiated GaN films, Look *et al.*[39] reported E_d values of 20.5 and 10.8 eV for Ga and N, respectively. Using MD methods, Nord *et al.*[25,38] also investigated the threshold displacement energy for Ga and N recoils in wurtzite GaN with 1000 random directions; they reported that the minimum E_d for gallium is obtained toward the second nearest Ga neighbor on the negative side of the c axis, and the smallest value for the threshold displacement energy for nitrogen is in a direction about 10° off the c axis. However, the calculated E_d value for Ga atoms is lower than that for N atoms in contrast to the experimental measurements. The lowest values for the threshold displacement energy were predicted to be 22 ± 1 for Ga and 25 ± 1 eV for N, and the average values are considerably high for N (109 ± 2 eV). In the present study, the average E_d value of 73.2 eV for gallium is considerably higher than that of 32.4 eV for nitrogen. The large discrepancy between the average values obtained from our simulations and those from classical MD simulations[25,38] may be a result of the fact that their simulations were performed in 1000 random directions, and in our work only five main crystallographic directions were considered. Another reason may be due to the different methods employed.

In conclusion, threshold displacement events along five main crystallographic directions in gallium nitride have been investigated using *ab initio* MD. Threshold displacement energies have been determined for single events and the associated defect configuration has been identified. For the lim-

ited directions considered, the minimum Ed for Ga is 39 eV along the $\langle 10\bar{1}0 \rangle$ direction and the minimum Ed for N is 17.0 eV along the $\langle \bar{1}010 \rangle$ direction, which agree fairly well with experimental measurements. Based on the calculations from five main crystallographic directions considered, the average E_d value for gallium and nitrogen atoms is estimated to be 73.2 and 32.4 eV, respectively. In general, the average threshold displacement energy for Ga recoils is larger than that for N recoils, in contrast to the previously classic MD simulations with empirical potentials. All the N recoil events generate a similar defect configuration, i.e., a N–N dumbbell, whereas the Ga recoil events create a variety of different defect configurations.

ACKNOWLEDGMENTS

[1] S. J. Pearton, J. C. Zolper, R. J. Shul, and F. Ren, J. Appl. Phys. **86**, 1 (1999).
[2] S. O. Kucheyev, J. S. Williams, J. Zou, C. Jagadish, and G. Li, Nucl. Instrum. Methods Phys. Res. B **178**, 209 (2001).
[3] E. Wendler, A. Kamarou, E. Alves, K. Gärtner, and W. Wesch, Nucl. Instrum. Methods Phys. Res. B **206**, 1028 (2003).
[4] B. Park, W. J. Weber, and L. R. Corrales, Nucl. Instrum. Methods Phys. Res. B **166-167**, 357 (2000).
[5] G. Lucas and L. Pizzagalli, Phys. Rev. B **72**, 161202 (2005).
[6] H. H. Tan, J. S. Williams, J. Zou, D. J. Cockayne, S. J. Pearton, and R. A. Stall, Appl. Phys. Lett. **69**, 2364 (1996).
[7] N. Parikh, A. Suvkhanov, M. Lioubtchenko, E. Carlson, M. Bremser, D. Bray, R. Davis, and J. Hunn, Nucl. Instrum. Methods Phys. Res. B **127-128**, 463 (1997).
[8] C. Liu, B. Mensching, M. Zeitler, K. Volz, and B. Rauschenbach, Phys. Rev. B **57**, 2530 (1998).
[9] W. Jiang, W. J. Weber, S. Thevuthasan, G. J. Exarhos, and B. J. Bozlee, MRS Internet J. Nitride Semicond. Res. **4S1**, G6.15 (1999).
[10] W. R. Wampler and S. M. Myers, MRS Internet J. Nitride Semicond. Res. **4S1**, G3.73 (1999).
[11] S. O. Kucheyev, J. S. Williams, C. Jagadish, G. Li, and S. J. Pearton, Appl. Phys. Lett. **76**, 3899 (2000).
[12] S. O. Kucheyev, J. S. Williams, C. Jagadish, J. Zou, and G. Li, Phys. Rev. B **62**, 7510 (2000).
[13] C. Liu, A. Wenzel, B. Rauschenbach, E. Alves, A. D. Sequeira, N. Franco, M. F. d. Silva, J. C. Soares, and X. J. Fan, Nucl. Instrum. Methods Phys. Res. B **178**, 200 (2001).
[14] C. Björkas, K. Nordlund, K. Arstila, J. Keinonen, V. D. S. Dhaka, and M. Pessa, J. Appl. Phys. **100**, 053516 (2006).
[15] B. De Vries, A. Vantomme, U. Wahl, J. G. Correia, J. P. Araújo, W. Lojkowski, and D. Kolesnikov, J. Appl. Phys. **100**, 023531 (2006).
[16] B. Cui, P. I. Cohena, A. M. Dabiran, and R. Jorgenson, J. Appl. Phys. **98**, 083504 (2005).
[17] S. M. Myers and C. H. Seager, J. Appl. Phys. **97**, 093517 (2005).
[18] M. Katsikini, F. Pinakidou, and E. C. Paloura, J. Appl. Phys. **101**, 083510 (2007).
[19] C. Liu, B. Mensching, M. Zeitler, K. Volz, and B. Rauschenbach, Appl. Phys. Lett. **71**, 2313 (1997).
[20] A. Y. Polyakov, N. B. Smirnov, A. V. Govorkov, A. V. Markov, and S. J. Pearton, J. Vac. Sci. Technol. B **25**, 436 (2007).
[21] S. O. Kucheyev, J. S. Williams, C. Jagadish, J. Zou, and G. Li, Phys. Rev. B **64**, 035202 (2001).
[22] T. Diaz de la Rubia and G. H. Gilmer, Phys. Rev. Lett. **74**, 2507 (1995).
[23] M.-J. Caturla, T. Diaz de la Rubia, L. A. Marqués, and G. H. Gilmer, Phys. Rev. B **54**, 16683 (1996).
[24] K. Nordlund, M. Ghaly, R. S. Averback, M. Caturla, T. Diaz de la Rubia, and J. Tarus, Phys. Rev. B **57**, 7556 (1998).
[25] J. Nord, K. Nordlund, and J. Keinonen, Phys. Rev. B **65**, 165329 (2002).
[26] W. Windl, T. Lenosky, J. Kress, and A. Voter, Nucl. Instrum. Methods Phys. Res. B **141**, 61 (1998).
[27] J. Perlado, J. Nucl. Mater. **251**, 98 (1997).
[28] R. Devanathan, T. Diaz de la Rubia, and W. J. Weber, J. Nucl. Mater. **253**, 47 (1998).
[29] R. Devanathan and W. Weber, J. Nucl. Mater. **278**, 258 (2000).
[30] J. Perlado, L. Malerba, A. Sánchez-Rubio, and T. Diaz de la Rubia, J. Nucl. Mater. **276**, 235 (2000).
[31] L. Malerba and J. M. Perlado, Phys. Rev. B **65**, 045202 (2002).
[32] J. Koike, D. M. Parkin, and T. E. Mitchell, Appl. Phys. Lett. **60**, 1450 (1992).
[33] B. Park, W. J. Weber, and L. R. Corrales, Nucl. Instrum. Methods Phys. Res. B **166–167**, 357 (2000).
[34] B. Park, W. J. Weber, and L. R. Corrales, Phys. Rev. B **64**, 174108 (2001).
[35] B.-Y. Wang, Y.-X. Wang, Q. Gu, and T.-M. Wang, Comput. Mater. Sci. **8**, 267 (1997).
[36] F. Gao and D. J. Bacon, Philos. Mag. A **67**, 289 (1993).
[37] L. A. Zepeda-Ruiz, S. Han, D. J. Srolovitz, and R. Car, Phys. Rev. B **67**, 134114 (2003).
[38] J. Nord, K. Nordlund, J. Keinonen, and K. Albe, Nucl. Instrum. Methods Phys. Res. B **202**, 93 (2003).
[39] D. C. Look, D. C. Reynolds, J. W. Hemsky, J. R. Sizelove, R. L. Jones, and R. J. Molnar, Phys. Rev. Lett. **79**, 2273 (1997).
[40] E. Holmström, A. Kuronen, and K. Nordlund, Phys. Rev. B **78**, 045202 (2008).
[41] J. M. Soler, E. Artacho, J. D. Gale, A. Garcia, J. Junquera, P. Ordejon, and D. S. Portal, J. Phys.: Condens. Matter **14**, 2745 (2002).
[42] N. Troullier and J. L. Martins, Phys. Rev. B **43**, 1993 (1991).
[43] L. Kleinman and D. M. Bylander, Phys. Rev. Lett. **48**, 1425 (1982).
[44] H. A. H. AL-Brithen, R. Yang, M. B. Haider, C. Constantin, E. Lu, and A. R. Smith, Phys. Rev. Lett. **95**, 146102 (2005).
[45] D. R. Lide, *Handbook of Physics and Chemistry* (CRC, New York, 1995).
[46] J. Perdew and A. Zunger, Phys. Rev. B **23**, 5048 (1981).
[47] H. Y. Xiao, X. T. Zu, F. Gao, and W. J. Weber, J. Appl. Phys. **103**, 123529 (2008).
[48] F. Gao, E. J. Bylaska, and W. J. Weber, Phys. Rev. B **70**, 245208 (2004).
[49] A. Ionascut-Nedelcescu, C. Carlone, A. Houdayer, H. J. v. Bardeleben, J.-L. Cantin, and S. Raymond, IEEE Trans. Nucl. Sci. **49**, 2733 (2002).